ORGANIC PROCESS RESEARCH & DEVELOPMENT
OPR&D

Full Paper

Process Safety Considerations for the Supply of a High Energy Oxadiazole IDO1-Selective Inhibitor

Theodore A Martinot, Michael J. Ardolino, Lu Chen, Yu-hong Lam, Chaomin Li, Matthew L Maddess, Daniel J. Muzzio, Ji Qi, Josep Saurí, Zhiguo Jake Song, Lushi Tan, Thomas P. Vickery, Jingjun Yin, and Ralph Zhao

Org. Process Res. Dev., **Just Accepted Manuscript** • DOI: 10.1021/acs.oprd.9b00105 • Publication Date (Web): 28 May 2019

is published by the American Chemical Society. 1155 Sixteenth Street N.W., Washington, DC 20036

Process Safety Considerations for the Supply of a High Energy Oxadiazole IDO1-Selective Inhibitor

Theodore A. Martinot,[*,†,※] *Michael Ardolino,*[†] *Lu Chen,*[⊥] *Yu-hong Lam,*[‡] *Chaomin Li,*[†,⌂] *Matthew L. Maddess,*[†] *Daniel Muzzio,*[§] *Ji Qi,*[§] *Josep Saurí,*[†] *Zhiguo J. Song,*[§] *Lushi Tan,*[§] *Thomas Vickery,*[§] *Jingjun Yin,*[§] *and Ralph Zhao*[§]

AUTHOR ADDRESS

[†]Process Research & Development, MRL, Merck & Co., Inc., Boston, Massachusetts, 02115, USA

[§]Process Research & Development, MRL, Merck & Co., Inc., Rahway, New Jersey 07065, USA

[‡]Modeling and Informatics, MRL, Merck & Co., Inc., Rahway, New Jersey 07065, USA

⊥WuXi AppTec, 288 Fute Zhong Road, Waigaoqiao Free Trade Zone, Shanghai

200131, China

TOC GRAPHIC

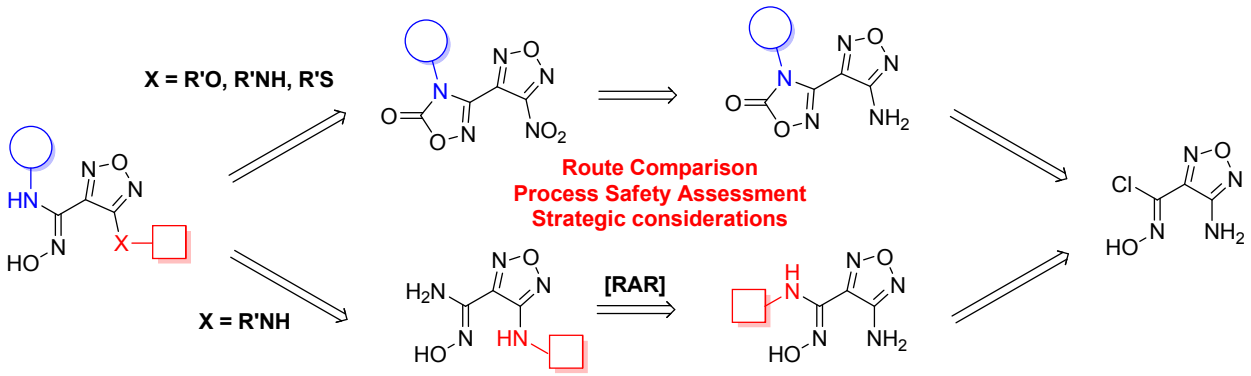
X = R'O, R'NH, R'S
X = R'NH
[RAR]
Route Comparison
Process Safety Assessment
Strategic considerations

ABSTRACT: The development of a stereospecific synthesis of a IDO1-selective inhibitor is described. The synthetic strategy towards enabling early discovery efforts along with additional findings pertaining to process safety which limited scalability are outlined. A convergent approach that supported the synthesis of material suitable for early pre-clinical and/or GLP toxicology studies, and which avoided the formation of key high energy intermediates is summarized.

KEYWORDS: Process Safety, Oxadiazole, Benzocyclobutylamine, IDO1

INTRODUCTION

Continued interest in immuno-oncology has been spurred by the demonstrated durable responses observed in patients treated with anti-PD1 mAb (e.g., pembrolizumab), among other therapies.[1] Indoleamine-2,3-dioxygenase-1 (IDO1) has been shown to play an important role in immunomodulation.[2] Moreover, IDO1 is over-expressed in multiple tumor types (including melanoma, colon, and ovarian), and this mechanism is believed to contribute to immunosuppression, which in turn may promote tolerance to the cancer.[3,4] The combination of IDO1 inhibitors and anti-PD1 mAbs has been shown to be synergistic in efficacy models,[5] and multiple clinical trials are currently evaluating the efficacy of this combination as a means of improving response rates while maintaining durability.

Notably, epacadostat (INCB24360; **1**, Figure 1)[6] has been developed to this end, and is currently being evaluated in multiple clinical trials in combination with anti-PD1 mAb therapy (pembrolizumab, nivolumab, etc.). Additional IDO1 inhibitors have been developed and reported upon in the literature.[7]

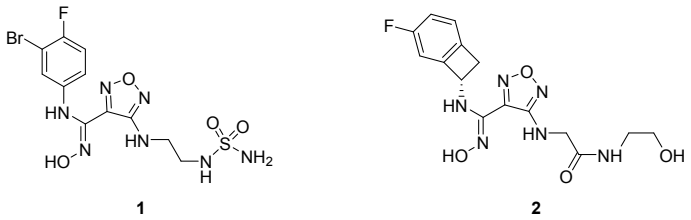

Figure 1. Structure of epacadostat (**1**) and **2**

Recently, we sought a synthetic approach to structures such as **2** that enabled the discovery effort around this target (IDO1) and facilitated the construction of Structure-Activity Relationship (SAR) around both sides of the oxadiazole.[7] The following discussion will feature strategic elements surrounding the supply of **2**, including route planning with regards to availability of the building blocks and safety, as well as impact of the selection of these building blocks or intermediates on the delivery timeline.

INITIAL ROUTE TO **1** AND PRELIMINARY EVALUATION

Initial access to **2** (Scheme 1) started from benzocyclobutyl carboxylic acid **3**, which was initially available in small quantities, and converted to the amine using a Curtius rearrangement.[7] Initial efforts to support SAR for this target (IDO1) carried the racemic carbamate (**rac-4**) forward, with a resolution of the final inhibitor (e.g., **2**), typically using supercritical fluid chromatography with a chiral stationary phase ("chiral SFC").

However, once the configuration of the optimal benzocyclobutylamine building block was determined to be (*S*), this intermediate was amenable to early resolution, which facilitated downstream operations by avoiding resolution of each new compound. The racemic *N*-Boc amine was resolved using chiral SFC to afford **4**. After deprotection to afford the benzocyclobutylamine hydrochloride salt (**5•HCl**), hydroxyamidine **7** was formed by condensation with commercially-available imidoyl chloride **6**.[8] The hydroxyamidine was protected as the cyclic carbamate by reaction with carbonyldiimidazole (CDI), and the amino-oxadiazole (**8**) was oxidized to the nitro-oxadiazole (**9**) using hydrogen peroxide in trifluoroacetic acid (TFA) or sulfuric acid.[9] The final product was obtained by condensation of the ethanolamine side chain (**10**) through displacement of the nitrooxadiazole and subsequent deprotection of the carbamate.

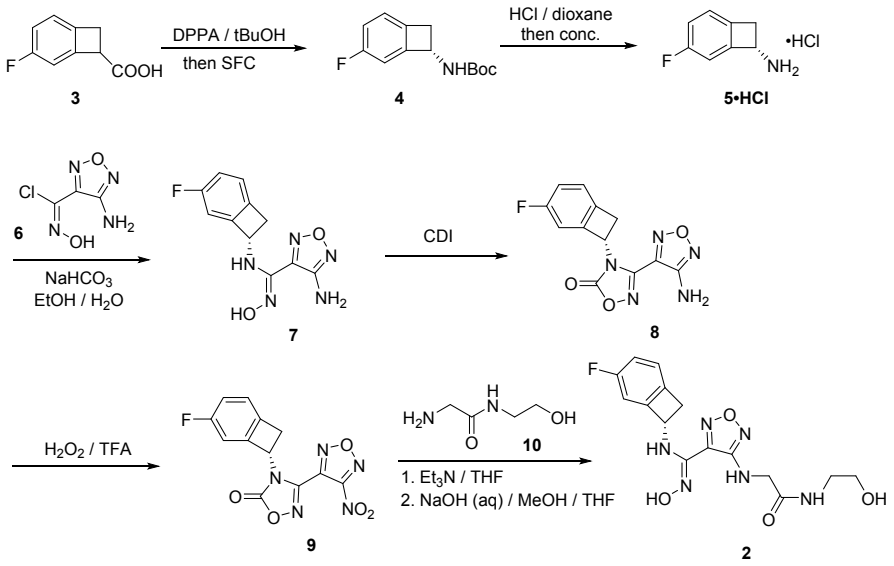

Scheme 1. Initial route to **2**

A significant advantage of the route outlined in Scheme 1 is that intermediate **9** was a versatile building block for rapidly enabling SAR evaluation of the tailpieces, with the nitro group being a suitable leaving group for a variety of nucleophiles (amine, alcohol, thiol, etc.).[10] However, the route was also limiting in that the stereogenic and arguably more precious portion of the molecule was installed first. This produced a potential bottleneck, as availability of benzocyclobutylamine **5** was limited early on in the program. Moreover, the safety element associated with handling compounds **8** and particularly **9** were a concern because of the low carbon-count relative to the number of

heteroatoms (e.g., in **8**) or relative to the number of energetic functional groups in the molecule (oxadiazole, nitro, etc. in **8** and **9**).[11,12]

Differential Scanning Calorimetry (DSC) was used as a primary means of evaluating and triaging intermediates of concern. Specifically, amino-oxadiazole **8** was first analyzed by DSC (Figure 2) and showed a clean melt with an onset at 213.9 °C, followed by an exothermic decomposition, which is attributed primarily to decomposition of the oxadiazole and/or the benzocyclobutylamine. The integrated heat for this decomposition, which has an onset of 254 °C, is 1567 J/g, which is considered significant.[13] Drop weight tests were performed on **8** at up to 30 J, and were negative (6 of 6 drop tests), indicating that the compound was not shock-sensitive. The high onset of decomposition (both absolute and relative to a reaction temperature of 25 °C), coupled with the apparent high crystalline nature of the intermediate (indicated by the sharp melt) led us to conclude that **8** was an intermediate that could be synthesized and handled safely at intermediate scale (< 1 kg), as both the melt and the decomposition occur more than 100 °C above the highest achievable reaction temperature.[14]

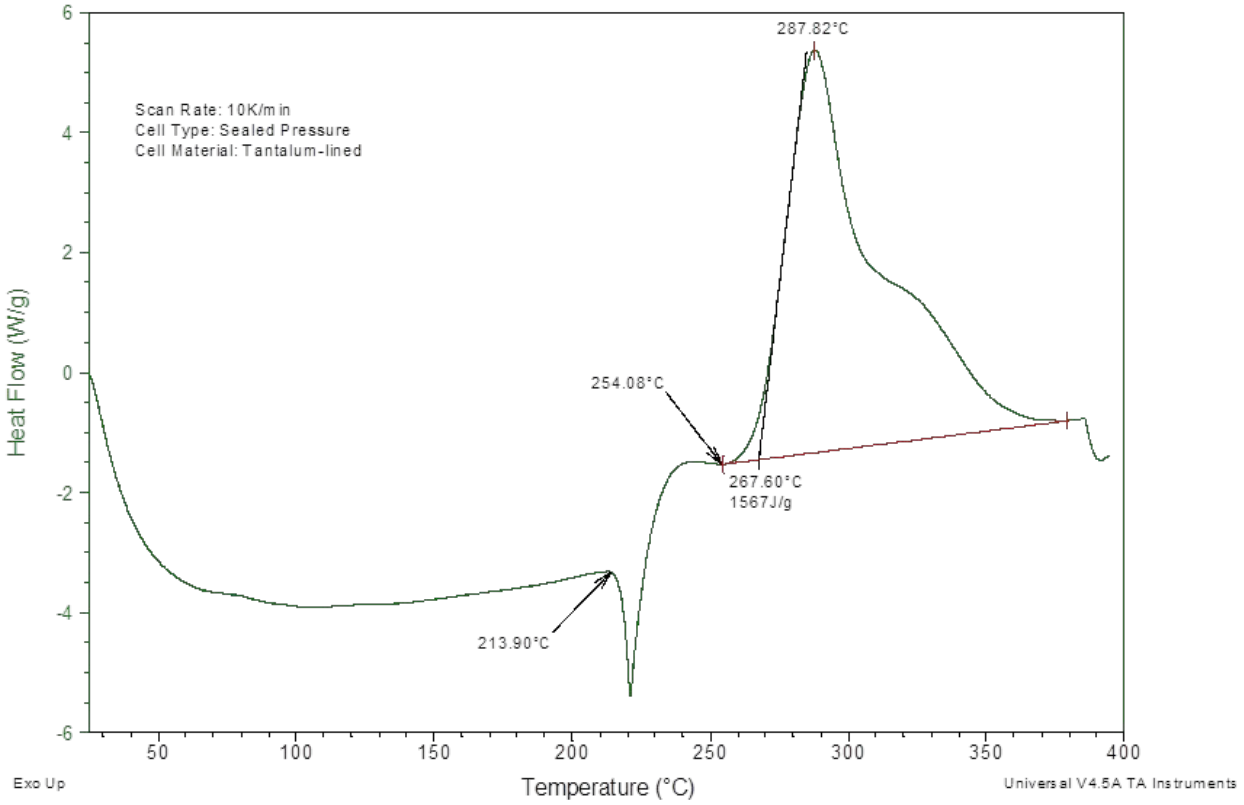

Figure 2. DSC thermogram of **8** (sample size: 5.70 mg)

A similar evaluation of **9** was conducted, but the DSC of the nitro-oxadiazole was shown to be significantly different (Figure 3). In this case, the intermediate showed a lower onset temperature for its melt (of approx. 87 °C) relative to its precursor (**8**), and that transition was also poorly defined. Following its melt, the compound showed a decomposition exotherm with an onset of 109 °C, and an integrated heat of decomposition of >3000 J/g; it is noted that the onset of each these transitions is a best

case scenario, as solutions or impure phases with no melting obstacles. Drop weight tests of **9** gave 3 of 6 positive results at 30 J impact (decomposition (charring); no smoke, flame or audible report), but no positive results at 20 J intensity. Combined, these results constituted a significant safety risk for scale-up. Therefore, a better understanding of the synthetic process to the formation of **9** was deemed necessary in order to fully evaluate whether the approach to **2** outlined in Scheme 1 could be safely conducted.

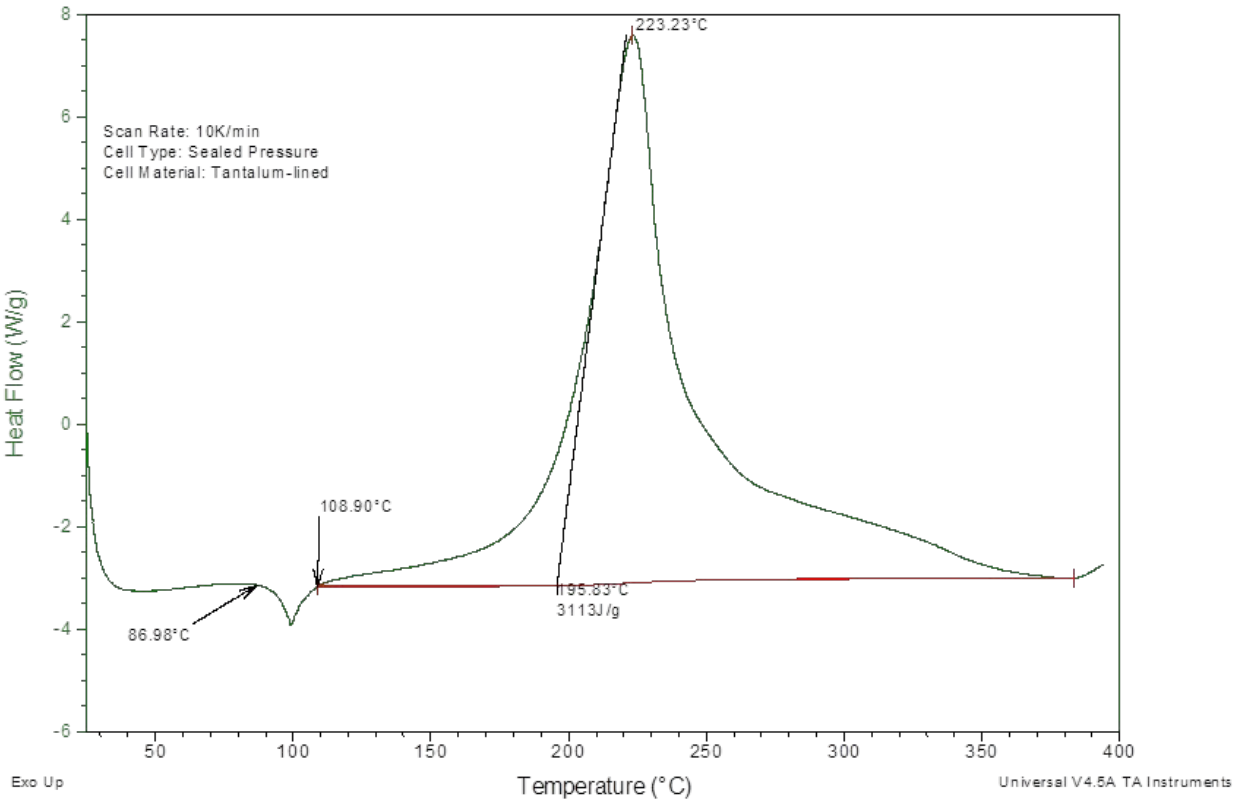

Figure 3. DSC thermogram of **9** (sample size: 3.40 mg)

FORMATION OF **9**

The conversion of **8** to **9** can be effected by a number of different reaction conditions. The "Piranha" (sulfuric acid / hydrogen peroxide[16]) conditions[9] were evaluated, but resulted in a complex mixture, and alternative options were therefore considered. After some additional evaluation, it was determined that either trifluoroacetic acid (TFA)[17] / urea hydrogen peroxide (UHP)[18] or TFA / hydrogen peroxide afforded the cleanest reaction profile. Both sets of conditions are believed to proceed through the same reactive species (pertrifluoroacetic acid, PTFA[19,20,21]), therefore selection of conditions was based on more practical considerations. Further development led to the conclusion that the latter set of conditions using hydrogen peroxide was likely easier to operate because hydrogen peroxide can be dosed continuously more easily than UHP (a solid), which in turn means that the individual reaction steps could be better controlled, thus avoiding potential runaway exotherms.

The main impurity of the reaction is nitrile oxime **11** (Scheme 2), which is believed to originate from the condensation of the intermediate nitroso-oxadiazole with the starting material (**8**) followed by degradation of the corresponding diazo-oxadiazole dimer.[15]

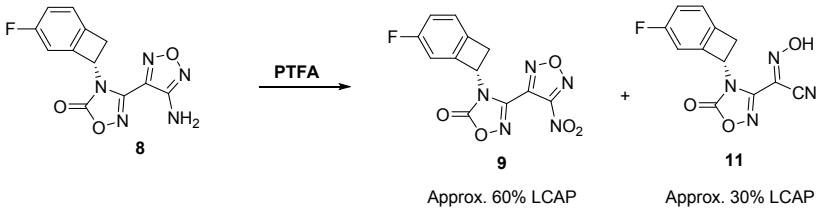

Scheme 2. Oxidation of **8** to **9**

Empirically, only **8**, **9**, and **11** have been observed (by HPLC-MS analysis) over the course of the reaction; therefore, it is believed that the relative rate for the initial oxidation to the hydroxylamine must therefore be a rate-determining step (i.e., no appreciable accumulation of the hydroxylamine or nitroso intermediates) and the formation of **11** as a byproduct of the reaction may be inevitable under these reaction conditions unless the mechanism for the formation of **9** itself were to be changed. Indeed, varying the reaction temperature, concentration, hydrogen peroxide addition rate, or stoichiometry did not have a statistically-significant effect on the ratio of **11** to **9** at the end of the reaction. While reaction temperature was shown to have an effect on

the reaction conversion, there was no statistically-significant variation in the amount of impurity relative to the product under any of the conditions tested. This observation indicates that formation of the impurity under the reaction conditions used may not be easily suppressed. Fortunately, upon completion of the reaction, the reaction mixture is diluted with water, which causes the desired product (**9**) to nucleate, and most of the impurities (including **14**) can be purged through the mother liquor.

In addition, reaction calorimetry for the oxidation of **8** to **9** was performed (both in a SuperCRC™ calorimeter and in a Mettler Toledo EasyMax™ equipped with the HFCal™) to determine safe operating conditions. First, the addition of hydrogen peroxide to TFA was evaluated. From the data collected in the EasyMax™, it was determined that the enthalpy associated with the addition of 0.10 mol of hydrogen peroxide to 0.78 mol of TFA and the subsequent formation of PTFA is approximately 1 kJ, which corresponds to an adiabatic temperature rise (ΔT_{ad}) of < 10 K. Moreover, because this exotherm is addition-controlled with no apparent thermal accumulation or delay, the risk posed to the operator in terms of a runaway exotherm can be minimized.

Separately, the enthalpy measured in the EasyMax™ for the oxidation reaction conducted on 3 g (0.010 mol) of **8** with 0.10 mol of hydrogen peroxide was determined to be approx. 6 kJ when the reaction was run at ≤ 40 °C, but increased to 16 kJ when the same reaction was run at 60 °C. These reaction enthalpies correspond to a ΔT_{ad} of 40 K and 120 K, respectively. In the CRC, the same reactions performed at 25 °C and 40 °C produced ΔT_{ad} of 9 K and 90 K, respectively. Though the absolute magnitude of these temperature rises do not match absolutely, the trends are compelling, and this remarkable increase in reaction enthalpy for the higher temperature experiments appears to be caused by the acceleration of the degradation of PTFA as a function of temperature. Finally, Accelerating Rate Calorimetry (ARC) performed on this reaction following a rapid addition of hydrogen peroxide showed a significant temperature and pressure increase at approx. 50 °C, which was also indicative of a potential runaway exotherm due to PTFA degradation (Figure 4).

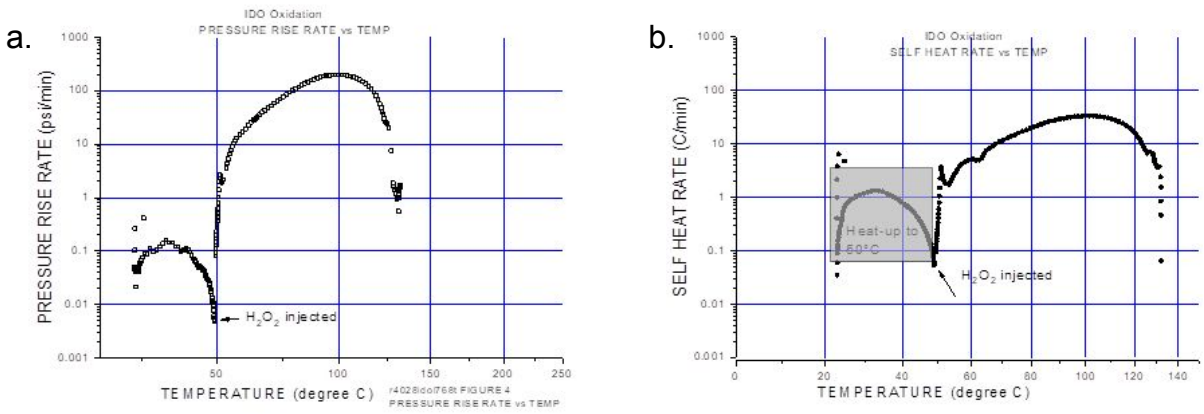

Figure 4. ARC data showing Self Heat Rate (a) and Pressure Rise Rate (b) as a function of temperature for the oxidation of **8** to **9**. Experiments were performed by dissolving **8** in TFA and heating to 50 °C, then injecting H_2O_2 at once (see annotation) with the ARC in adiabatic tracking mode.

These data as a whole indicate that care should be taken when performing this oxidation in order to avoid the thermal decomposition of the PTFA formed. Based on the results collected, as well as the lack of benefit of performing this oxidation at significantly higher temperature (Figure 5), the recommended batch temperature is ≤ 45 °C at intermediate scale (< 200 g) with a slow dosing of hydrogen peroxide: Although this temperature is close to the potential degradation of the PTFA, the slow dosing of

hydrogen peroxide allows for minimal accumulation of this reagent, and accelerates the rate of oxidation, thereby minimizing risk to the operator. It is recognized that the edge of failure for this runaway reaction has not been systematically confirmed (i.e., the temperature at which the PTFA degradation will cause the reaction to self-heat), and for this reason, alternative strategies for the assembly of **2** were strongly considered in order to avoid going through this high energy intermediate and reaction.

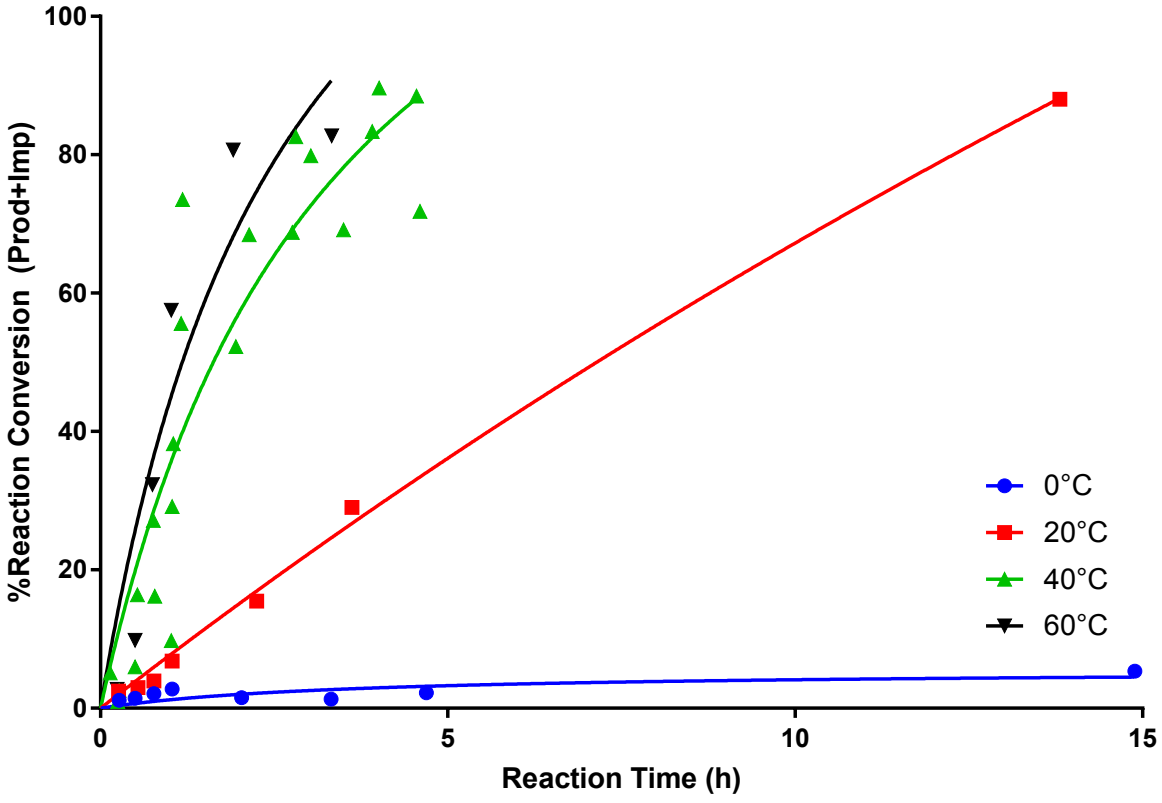

Figure 5. Effect of temperature on the reaction conversion of **8** to **9**

One final concern over the approach to **2** outlined in Scheme 1 is in the condensation of benzocyclobutylamine **5** with imidoyl chloride **6**. As noted elsewhere,[22,23] the nitrile oxide formed from treatment of imidoyl chloride **6** with base (**12**) can homodimerize to form the symmetrical dioxadiazene (**13**) and/or its isomeric oxadiazole oxide (**15**), depending on the reaction conditions used (Scheme 3). As expected, these species are highly energetic, and their corresponding oxidation products (**14** and **16**) are known explosives.[22,23] While the outcome of the condensation of **5** and **6** seems to primarily result in the formation of **7**, we have not attempted to prove that neither **13** nor **15** are present in the isolated product from this reaction because synthesis of the corresponding markers and their handling is considered high risk. Therefore, **7** as well as **8** could technically contain these corresponding impurities, depending on the reaction parameters used. As a result of this known but uncharacterized risk, and the risk associated with the formation of nitro-oxadiazole **9**, an alternative approach to **2** was carefully evaluated.

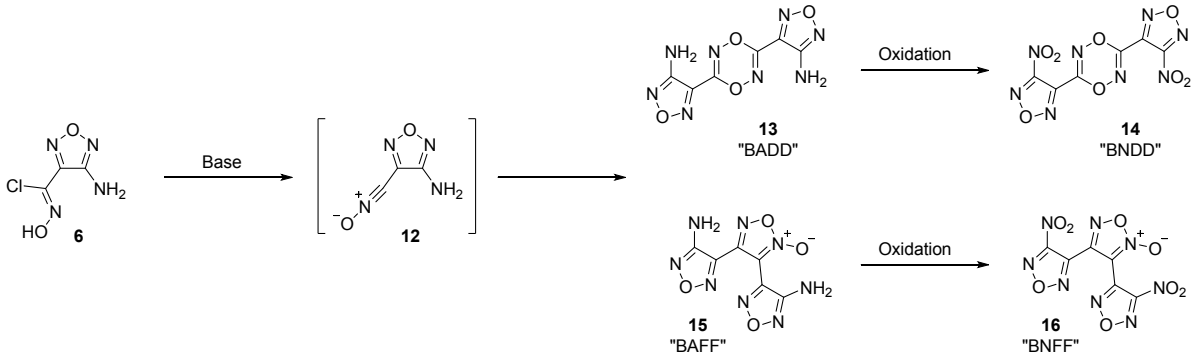

Scheme 3. Undesired dimerization of imidoyl chloride **6**[22,23]

IMPROVED ACCESS TO THE BENZOCYCLOBUTYLAMINE

Early on in development, the synthesis of benzocyclobutylamine **5** was optimized to allow access to kilogram quantity of the desired product using the existing route. Most notable in the improved synthesis is the classical resolution of the benzocyclobutylamine,[24] which obviated the need for costly SFC of this intermediate. Indeed, the Process Mass Intensity (PMI) for the Curtius rearrangement step and the SFC resolution alone in the original approach was estimated at 3839 due to the high material demand (solvent and CO_2) of the chromatography. In contrast, the process outlined in Scheme 4 decreased the PMI for the Curtius rearrangement and classical

resolution to 98.7. While the resulting PMI is still relatively high for a single step, the approach was deemed fit-for-purpose at this stage in development.

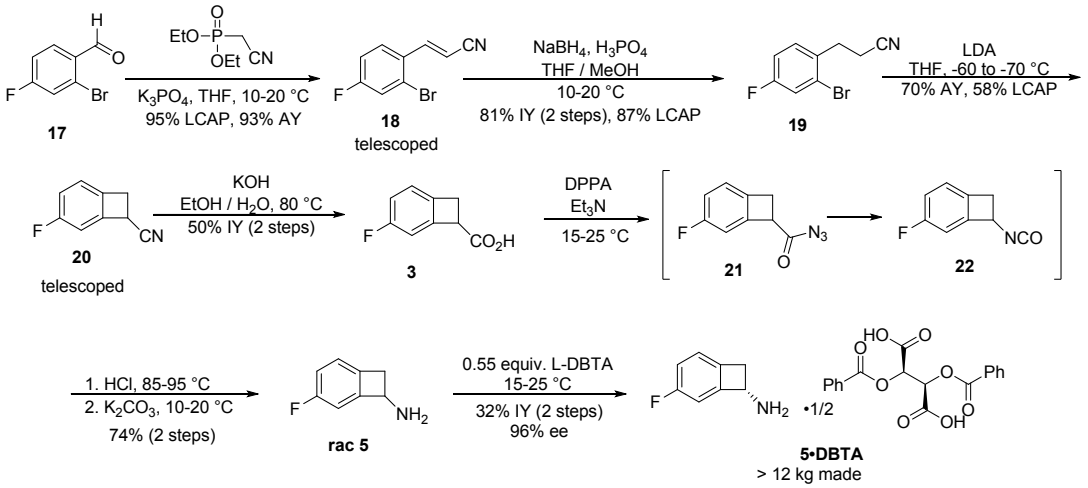

Scheme 4. Synthesis of benzocyclobutylamine **5** on kilogram scale

APPROACH TO 2 VIA OXADIAZOLE REARRANGEMENT

To enable a safer supply of **2**, an approach that takes advantage of the previously-demonstrated[6] Boulton-Katritzky rearrangement (RAR) was attempted (Scheme 5). This approach provides a number of benefits over the initial approach shown in Scheme 1, namely: [1] the route is more convergent; [2] the hydroxyamidine functionality does not need to be protected; [3] with the exception of imidoyl chloride **6**, no exceedingly high

energy intermediates are used; [4] the benzocyclobutylamine **5** is introduced late, which results in a higher overall throughput when this material was of limited availability.

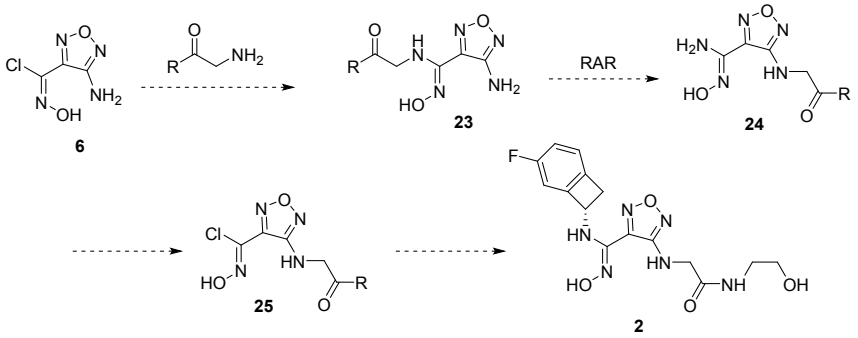

Scheme 5. Revised strategy to **2**

However, it was determined that under the conditions needed to effect the oxadiazole rearrangement on our substrate (aq. KOH, 100 °C),[6] the ethanolamine amide in the fully-elaborated tailpiece is hydrolyzed. A screen aimed at finding non-aqueous conditions that effect this rearrangement failed to afford conditions that were competitive. As a result, a modified strategy was implemented that still installed the hydroxyamidine first, but with a sacrificial ester that would get saponified during the rearrangement conditions (Scheme 6). To better understand the thermodynamics of the transformation, the starting acid (**28**) and product (**29**) were modeled. From the analysis

performed, it is determined that the rearrangement is thermodynamically-favored (ΔG_{rxn}= -3.9 kcal/mol), and that the geometry of the hydroxyamidine is very important to the conformation of the starting material and product, with the (*Z*)-isomer being favored in both cases. Therefore, because the mechanism of the Boulton-Katritzky rearrangement is believed to be concerted, these data suggest that the starting oxime ((*Z*)-**28**, presumably as the dianion due to the high pH of the reaction mixture) must first isomerize prior to rearrangement to the less favored (*E*)-isomer which then has the proper geometry to enable the rearrangement. The product of the rearrangement then will undergo isomerization to the final most stable conformer, (*Z*)-**29** (Scheme 6), and it is the release of energy from the combined rearrangement and isomerization that makes the rearrangement favorable thermodynamically.

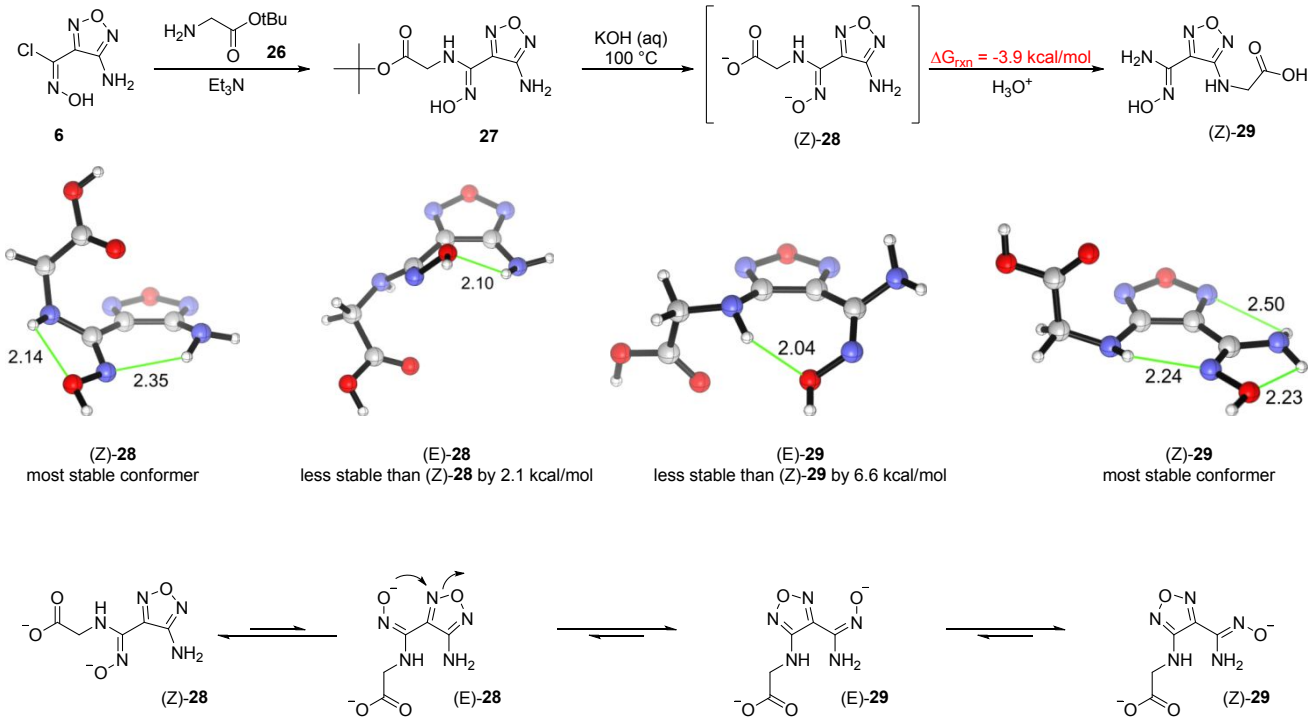

Scheme 6. Installation of the tailpiece and rearrangement as well as computed energies for the rearrangement (M06-2X-D3/6-311G(d,p)–SMD(water) geometries and frequencies. M06-2X-D3/def2-QZVPP–SMD(water) single-point energies.)

The optimized synthesis of **2** is provided in Scheme 7. The formation of hydroxyamidine **27** proceeded smoothly, with the product being isolated by direct crystallization from ethyl acetate. The hydrolysis and rearrangement of **27** affords **29** cleanly, although it does require a 48 h reaction time. Acid **29** is also isolated directly from the reaction mixture after neutralization, thus facilitating the process steps.

However, the condensation of **29** with **30**[25] to complete the tailpiece assembly was problematic at first, with varying yields of product being obtained, and unreliable outcomes requiring complex chromatography.

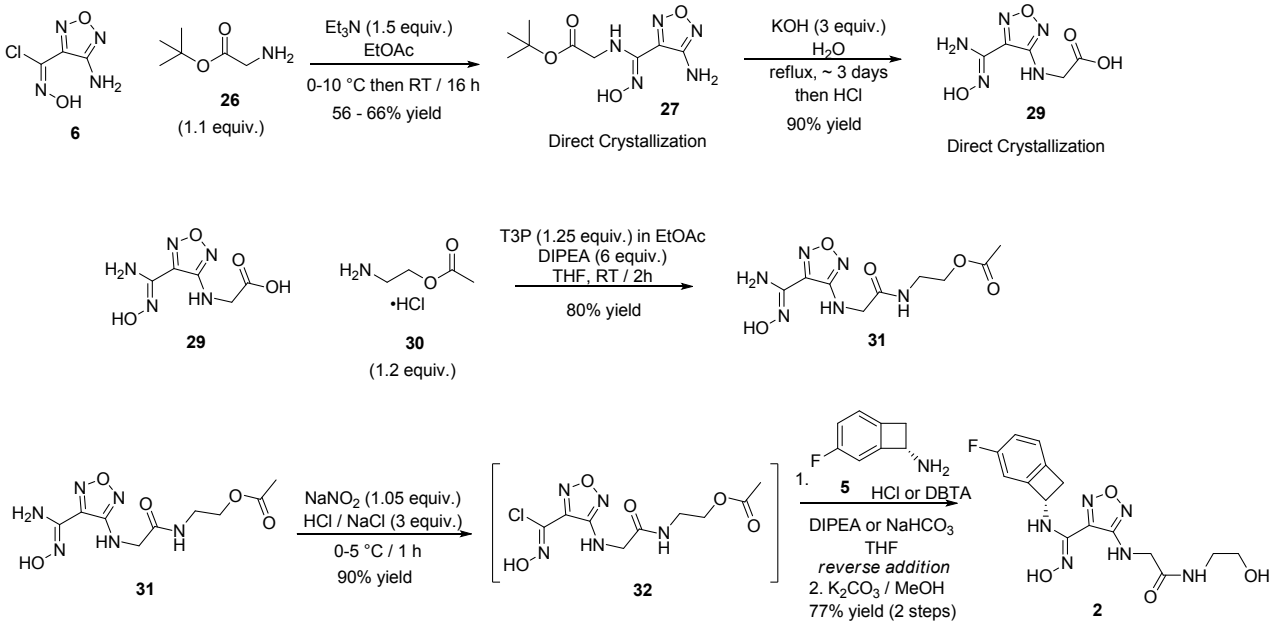

Scheme 7. Final delivery approach

Initially, EDC and HOBt were used as coupling reagents, but product **31** proved difficult to separate from HOBt and related reagents, thereby limiting the use of many common amide-coupling reagents.[26] Small-scale runs had shown propylphosphonic anhydride (T3P) to be a favorable amide coupling reagent for the transformation.

However, upon repeated reactions and increase in scale, multiple byproducts including the pseudo-dimer **33** (Figure 6) were observed, resulting in low yield and purity of **31**.

In order to quickly identify the key parameters driving reaction efficiency and cleanliness, a Design of Experiments (DoE) approach was taken. For this, a 24-experiment design was initially created using the JMP software.[27] The design allowed use of a common 24-well plate array (1 mL shot vials) to facilitate reaction setup and analysis while minimizing starting material consumption, and evaluated 4 parameters: solvent (THF, DCM and EtOAc), DIPEA charge (2 – 4 equiv.), T3P charge (0.5 – 1.5 equiv.), and amine hydrochloride **30** charge (0.9 – 1.2 equiv.). Following completion of these experiments, analysis indicated that the DIPEA charge was insufficient, even at 4 equiv. Therefore, the DoE was augmented with 5 additional reactions to probe the effects of higher DIPEA (up to 8 equiv.). The model generated from the data collected showed DIPEA and T3P equivalents to be the main drivers of purity (panel I, Figure 6), with THF showing the best balance of conversion and purity among the solvents. Setting response levels at >80% conversion, >95% purity of converted product and <5% LCAP **33**, the contour profile (panel II, Figure 6) predicted a T3P loading of 1.25

equivalents and 6 equivalents of DIPEA with THF as the solvent to be ideal. Mechanistically, this makes sense, but was not obvious to us *a priori*: Each equivalent of T3P can generate, over the course of the reaction, up to 3 equiv. of phosphonic acid (therefore, the total base needed becomes: 3 x 1.25 (T3P) + 1 (amine HCl **30**) + 1 (acid **29**) = 5.75 ~ 6). With insufficient base, the amine becomes inaccessible (protonated) as the reaction proceeds and therefore the hydroxyamidine oxygen becomes the next possible nucleophile and results in the formation of **33**.

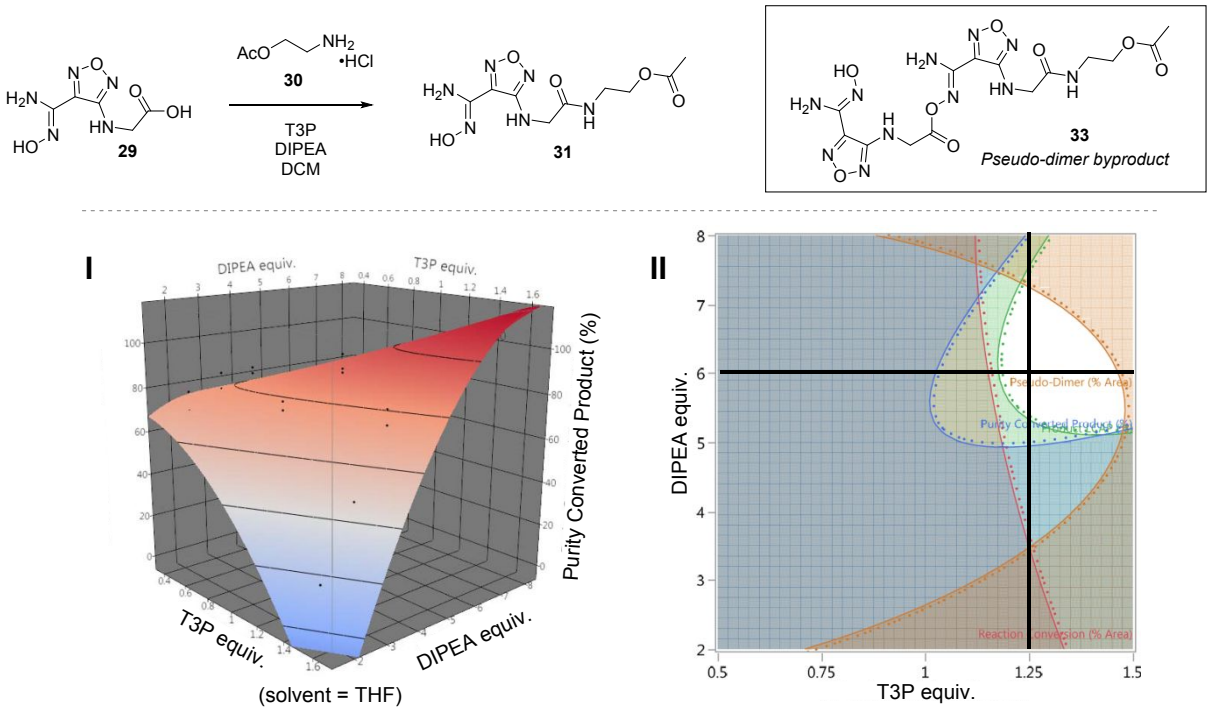

Figure 6. Optimization of the formation of **31**

These conditions were applied to the overall delivery of **2** (approx. 200 g scale; Scheme 7), allowing for a cleaner reaction, which after crystallization afforded **31** with high purity and yield. The optimized conditions demonstrated a robust design space across a wide scale range (~ mg in DoE optimization to > 200 g).

From **31**, the synthesis is completed by diazotization of the hydroxyamidine and *in situ* formation of imidoyl chloride **32**, followed by installation of **5** and deprotection of the tailpiece. As was observed for the formation of hydroxyamidine **8**, some dimerization may occur if the order of addition is reversed (Scheme 8): Namely, if imidoyl chloride **32** is pre-mixed with the salt of **5** (either HCl or DBTA), then base is added, the deprotonation of the imidoyl chloride appears to occur faster than the neutralization of the salt of **5** (i.e., the neutralization reaction may be mass-transfer limited due to solubility limitations), and therefore results in formation of the corresponding nitrile oxide, which was found to effectively homodimerize (Scheme 8). The solution to afford clean coupling is to first neutralize **5** by pre-mixing the salt with the base in the reaction solvent, and then adding in the imidoyl chloride solution from the previous step. After

final deprotection, the desired product (**2**) is obtained in approx. 70% yield over three steps from **31**.

Scheme 8. Homodimerization of **32**

CONCLUSION

A fit-for-purpose synthesis of high energy oxadiazole-bearing molecules has been evaluated. Taking advantage of the Boulton-Katritzky rearrangement the new approach enabled not only a more convergent route that allowed for the late-stage installation of the chiral building block **5**, but also avoided the generation of high energy intermediates such as nitrooxadiazole **9**. The optimized approach culminates in a longest linear sequence of nine (9) steps – several of which are telescoped – from commercially-available aldehyde **17**. This work ultimately enabled the safe synthesis of **2** in quantities sufficient to support toxicology studies.

EXPERIMENTAL SECTION

All reactions were carried out under a nitrogen atmosphere. All solvents and reagents were purchased from commercial sources and were used without further purification. ^{1}H NMR chemical shifts are reported relative to residual proton solvent peaks or TMS.

(S)-3-(4-amino-1,2,5-oxadiazol-3-yl)-4-(4-fluorobicyclo[4.2.0]octa-1(6),2,4-trien-7-yl)-1,2,4-oxadiazol-5(4H)-one (8). To a 5 L 4-neck round-bottomed flask, were charged (S)-4-fluorobicyclo[4.2.0]octa-1,3,5-trien-7-amine hemi L-dibenzoyl tartaric acid salt (**5•DBTA**) (435 g, 1.38 mol, 1.00 equiv) and hydrogen chloride in 1,4-dioxane (4500 mL of 4 M solution; 18 mol, 13.0 equiv.). The resulting mixture was stirred overnight at room temperature. The solids were collected by filtration. This resulted in 200 g (crude) of (S)-4-fluorobicyclo[4.2.0]octa-1,3,5-trien-7-amine hydrochloride as a white solid. Into a 10-L 4-neck round-bottomed flask, was charged sequentially a solution of (S)-4-fluorobicyclo[4.2.0]octa-1,3,5-trien-7-amine hydrochloride (200 g, 1.15 mol, 1.00 equiv) in acetonitrile (2000 mL, 10 vol.), a solution of sodium hydroxide (61 g, 1.53 mol, 1.30 equiv) in water (2000 mL, 10 vol.), a solution of (E)-4-amino-N-hydroxy-1,2,5-oxadiazole-3-carbonimidoyl chloride (**6**) (191 g, 1.18 mol, 1.00 equiv) in acetonitrile

(2000 mL, 10 vol.), a solution of potassium phosphate dibasic (302 g, 1.41 mol, 1.20 equiv) in water (1000 mL, 5 vol.), and the mixture was stirred at ambient temperature. After confirming that the initial condensation was complete per analysis of the reaction mixture by HPLC, charged diisopropylethylamine (190 g, 1.47 mol, 1.25 equiv), and CDI (219 g, 1.53 mol, 1.30 equiv) sequentially while stirring at ambient temperature. The resulting solution was stirred for 1 h at ambient temperature. The reaction was then diluted with water (2000 mL, 10 vol.), which caused a precipiation of the product. The resulting solution was extracted with ethyl acetate (2 x 3000 mL; 2 x 15 vol.) and the organic layers were combined. The resulting mixture was washed with 1 M hydrochloric acid (aq) (2 x 1000 mL; 2 x 5 vol.), then dried over anhydrous sodium sulfate, and concentrated to dryness under reduced pressure. This resulted in 250 g (74%) of (S)-3-(4-amino-1,2,5-oxadiazol-3-yl)-4-(4-fluorobicyclo[4.2.0]octa-1(6),2,4-trien-7-yl)-1,2,4-oxadiazol-5(4H)-one (**8**) as a white solid. ^{1}H NMR (300 MHz, DMSO-d6) δ 7.22 – 7.01 (m, 3H), 6.58 (s, 2H), 5.79 (t, *J* = 4.0Hz, 1H), 3.66–3.51 (m, 2H) ppm; ^{19}F NMR (282 MHz, DMSO-d6) δ -113.1 ppm; MS: m/z calcd for $C_{12}H_9FN_5O_3$ ($M+H^+$) 290.1, found 290.1; $[\alpha]_D^{20}$ +32.5 ° (c = 0.22, MeCN).

(S)-4-(4-fluorobicyclo[4.2.0]octa-1(6),2,4-trien-7-yl)-3-(4-nitro-1,2,5-oxadiazol-3-yl)-1,2,4-oxadiazol-5(4H)-one (9). (S)-3-(4-amino-1,2,5-oxadiazol-3-yl)-4-(4-fluorobicyclo[4.2.0]octa-1(6),2,4-trien-7-yl)-1,2,4-oxadiazol-5(4H)-one (**8**) (55.27 g, 191 mmol, 1.00 equiv.) was charged to a 5 L 3-neck round-bottomed flask. The flask was equipped with an overhead stirrer, reflux condenser, and thermocouple probe, and inerted under nitrogen. Trifluoroacetic acid (1105 mL, 20 vol.) was charged and the resulting mixture was stirred and heated with a target internal temperature of 40 °C. The hydrogen peroxide solution (32% w/w) (183 ml, 1911 mmol, 10 equiv.) was charged to an addition funnel and added to the reaction mixture dropwise, maintaining a batch temperature < 45 °C throughout the addition. After the addition was complete, continued stirring at 40-45 °C until the starting material was no longer consumed by LCMS analysis (i.e., steady state). The heating mantle was removed and replaced with an ice/water bath. Water (2.8 L, 50 vol.) was added dropwise to the reaction mixture while maintaining a batch temperature of < 10 °C throughout. The product was isolated by filtration through a polyethylene filter. Solids were washed with water (approx. 500 mL / 10 vol.) twice, then an additional slurry wash was performed, followed by a final

displacement wash with water (each with approx. 500 mL / 10 vol. of water). Solids were deliquored, but not dried further. Nitrooxadiazole **9** was used as-is and stored cold. Yield: 31.6 g (52%, uncorrected). ^{1}H NMR (600 MHz, DMSO-d6) δ 7.25 – 7.19 (m, 1H), 7.17 (t, J = 8.9 Hz, 1H), 7.10 (d, J = 7.3 Hz, 1H), 5.67 – 5.61 (m, 1H), 3.63 (d, J = 14.2 Hz, 1H), 3.48 (dd, 1H) ppm.

3-(2-bromo-4-fluorophenyl)propanenitrile (19). 2-Bromo-4-fluorobenzaldehyde (**17**; 200 kg, 985.2 mol, 1.00 equiv.) was charged to an appropriately-sized reactor (R1), followed by 2-methyltetrahydrofuran (500 kg, 2.5 wts.) and stirring was initiated to form a homogenous solution. Diethyl (cyanomethyl)phosphonate (194.2 kg, 1096.3 mol, 1.11 equiv.) was charged into a second appropriately-sized reactor (R2), followed by 2-methyltetrahydrofuran (681.8 kg, 3.4 wts.). Anhydrous K_3PO_4 (220.3 kg, 1037.8 mol, 1.05 equiv.) was charged to R2. While mixing the contents of R2, the solution prepared in R1 was transferred to R2 while maintaining the batch temperature of R2 at 10-15 °C. The contents of R2 were stirred at 10-15 °C for 4-6 h, and sampled for reaction completion by HPLC (residual aldehyde: 0.7%; target ≤ 3.0%). Water (586 kg, 2.9 wts.)

was charged to R2 and the mixture was stirred for 1 h, then stirring was stopped and the phases were allowed to separate (3 h). The aqueous phase was discarded. The organic phase was washed first with a mixture of 400 kg of 10% Na_2SO_4 (aq) and 50 kg of 10% H_3PO_4 (aq) (2.5 wts. total), then with 400 kg of 10% Na_2SO_4 (aq) (2.0 wts.). Solvent was exchanged to THF (total 1618 kg of THF was used) and the solution volume was reduced to approximately 1-2 volumes by distillation. THF (80 kg, 0.4 wts.), H_3PO_4 (4.4 kg, 0.022 wts.), and methanol (306.1 kg, 1.53 wts.) were charged sequentially to the reaction mixture, and the entire contents of the reactor were then transferred an auxilliary storage tank. To the empty reactor, sodium borohydride (99.8 kg, 2638.1 mol, 2.67 equiv.) and THF (900 kg, 4.5 wts.) were charged sequentially, and the batch temperature was adjusted to 10-20 °C. The solution from the storage tank was charged to the reactor containing the sodium borohydride solution over approx. 28 h, maintaining a batch temperature of 10-20 °C throughout, then maintained mixing for an additional 3 h at the same temperature once addition was complete. Reaction completion was monitored by HPLC. 10% H_3PO_4 (aq) (1.2 kg, 0.006 wts.) and MTBE (300 kg, 1.5 wts.) were charged to the reaction mixture sequentially, and the batch

temperature was increased to 20-30 °C. After stirring for 1 h, agitation was stopped, and the phases were allowed to separate for 2 h. The aqueous phase was drained and discarded. The organic phase was washed with a mixture of 7% $NaHCO_3$ (206 kg, ca. 1 wt.) and 10% Na_2SO_4 (614 kg, ca. 3 wts.). The organic phase was concentrated to approx. 1-2 volumes by distillation under reduced pressure, then MTBE (448.4 kg, 2.24 wts.) was charged and the organic phase was washed with 10% Na_2SO_4 (aq) (200 kg, 1 wt.). A solvent exchange to THF was performed (using 2142 kg of THF for the exchange) with a final target volume of 1-2 volumes, then the batch was diluted with THF (246 kg, 1.23 wt.). The organic phase (total weight: 692.6 kg) was assayed for product content: 26.5% w/w, with a purity of 87.1% a/a, corresponding to a yield of 183.5 kg (81.6%). Solution was used as-is for the subsequent transformation. Characterization data for **18**: ^{1}H NMR (400 MHz, $CDCl_3$) δ 7.99 (dd, *J* = 8.8, 5.8 Hz, 1 H), 7.46 (dd, *J* = 8.8, 5.8 Hz, 2 H), 7.08 (td, *J* = 8.3, 8.3, 2.5 Hz, 1 H), 5.52 (d, *J* = 11.8 Hz, 1 H) ppm; ^{13}C NMR (100 MHz, $CDCl_3$) δ 163.6 (br d, *J* = 255 Hz), 147.8, 130.0 (d, *J* = 4 Hz), 128.4 (d, *J* = 9 Hz), 125.3 (d, *J* = 10 Hz), 121.0 (d, *J* = 25 Hz), 117.5, 115.6 (d, *J* = 22 Hz), 99.0 (d, J = 3 Hz) ppm; ^{19}F NMR (100 MHz, $CDCl_3$) δ 106.4,106.6 ppm;

HRMS: m/z calcd for C9H5BrFN: (M+H+), 225.9662, Found: 225.9663 (M+ H+). Characterization data for **19**: ^{1}H NMR (400 MHz, $CDCl_3$) δ 7.30 (m, 2 H), 7.03 (td, *J* = 8.3, 8.3, 2.5 Hz, 1 H), 3.06 (t, *J* = 7.3 Hz, 2 H), 2.66 (t, *J* = 7.3 Hz, 2 H) ppm; ^{13}C NMR (100 MHz, $CDCl_3$) δ 161.6 (br d, *J* = 250.5 Hz) 133.2 (d, *J* = 3 Hz), 131.6 (d, *J* = 8 Hz), 124.0 (d, *J* = 10 Hz), 120.3 (d, *J* = 23 Hz), 118.7, 115.1(d, *J* = 10 Hz), 31.3, 17.7 (d, *J* = 1 Hz) ppm; ^{19}F NMR (100 MHz, $CDCl_3$) δ 112.5 ppm; HRMS: m/z calcd. for C_9H_7BrFN: ($M+H^+$), 227.9819, Found: 227.9820.

4-fluorobicyclo[4.2.0]octa-1,3,5-triene-7-carboxylic acid (3). THF (289.4 kg, 1.70 wts.) and diisopropylamine (238 kg, 2.35 mol, 3.13 equiv.) were charged to an appropriately-sized reactor (R1). The solution temperature was adjusted to a range of -20 °C to 10 °C. *n*-Butyllithium (2.5 M, 646 kg, 10.08 mol, 13.44 equiv.) was charged to the reactor while maintaining a batch temperature range between -20 °C and 10 °C (7 h addition time). The previously-prepared solution of 3-(2-bromo-4-fluorophenyl)propanenitrile (**19**; 643 kg of a 26.5% w/w solution, 170.4 kg, 0.75 mol, 1.00 equiv.) was charged into a separate appropriately-sized reactor (R2) followed by THF (680.6 kg, 4 wts.) and the

batch temperature was adjusted to -70 °C to -60 °C. The solution in R1 was added to the starting material in R2 while maintaining a batch temperature of -70 °C to -60 °C (9.5 h addition time), washing the transfer line with THF (19.2 kg, 0.1 wt.). The batch was stirred for 1 h and sampled for reaction completion (1% residual SM; target ≤ 5%). Water (122 kg, 0.72 wts.) was charged to R2 at -70 °C to -60 °C, and the batch was warmed to 10-25 °C. Water (510 kg, 3 wts.) was charged to R2, and then solvent was distilled off to a target volume of 3-4 volumes. Ethanol (300 kg, 1.76 wts.) was charged to R2, and then the batch was heated to 70-80 °C for 5 h, and subsequently cooled back down to 20-30 °C. Solvent was distilled off to a target volume of 2-3 volumes. Water (1360 kg, 8 wts.) and dichloromethane (1099.8 kg, 6.5 wts.) were charged to the reaction mixture, and the phases were mixed for 0.5 h, then allowed to settle (1 h). The organic phase was removed and discarded. The aqueous phase was transferred to another reactor (R3). Ethanol (402 kg, 2.4 wts.) was charged to R3 and the batch was warmed to 25-35 °C. 35% Hydrochloric acid (aq.) (206.8 kg, 1.21 wts.) was charged to R3 and the pH was checked (result: 1; target ≤ 3). The mixture was stirred for 2.5 h at 25-35 °C, then the batch cooled to 0-5 °C and stirred for an additional 1 h. The product

was isolated by filtration, washing the cake with water (300 kg, 1.8 wts.). The product was dried in a vacuum oven at 40-45 °C for 70 h. Yield: 72.25 kg of a brown solid with 87.3% area / 85.1% w/w purity (61.5 kg corrected), corresponding to a 50% corrected yield. Characterization data for **20**: ^{1}H NMR (400 MHz, $CDCl_3$) δ 7.08 (m, 2 H), 6.98 (m, 1 H), 4.22 (dd, *J* = 4.9, 2.6 Hz, 1 H), 3.64 (m, 1 H), 3.51 (m, 1 H) ppm; ^{13}C NMR (100 MHz, $CDCl_3$) δ 162.8 (br d, *J* = 249 Hz), 139.5 (d, *J* = 8 Hz), 138.1 (d, *J* = 3 Hz), 125.3 (d, *J* = 9 Hz), 119.0, 117.3(d, *J* = 24 Hz), 110.6(d, *J* = 24 Hz), 35.6, 28.1 (d, J = 3 Hz) ppm; ^{19}F NMR (100 MHz, $CDCl_3$) δ 110.7 ppm; HRMS: m/z calcd for C9H6FN: (M+H+), 148.0557, Found: (M+ H+): 148.0564. Characterization data for **3**: ^{1}H NMR (400 MHz, $CDCl_3$) δ 7.06 (t, *J* = 6.1, 6.1 Hz, 2 H), 6.96 (m, 2 H), 4.31 (t, *J* = 3.9, 3.9 Hz, 1 H), 3.44 (br d, *J* = 3.01 Hz, 2 H) ppm; ^{13}C NMR (100 MHz, $CDCl_3$) δ 178.4, δ 162.7 (br d, *J* = 244 Hz), 142.7 (d, *J* = 8 Hz), 139.0 (d, *J* = 3 Hz), 124.6 (d, *J* = 9 Hz), 116.0 (d, *J* = 24 Hz), 110.7 (d, *J* = 23 Hz), 44.8 (d, *J* = 3 Hz), 33.3 ppm; ^{19}F NMR (100 MHz, $CDCl_3$) δ 112.5 ppm; HRMS: m/z calcd for $C_9H_7FO_2$: ($M+H^+$), 167.0503, Found: 167.0514.

4-fluorobicyclo[4.2.0]octa-1,3,5-trien-7-amine (rac 5). 4-fluorobicyclo[4.2.0]octa-1,3,5-triene-7-carboxylic acid (**3**; net 61.5 kg, 370 mol, 1.00 equiv.) was charged to an appropriately-sized reactor (R1) followed by toluene (826 kg, 13.4 wts.) and the batch temperature was adjusted to 10-20 °C. Triethylamine (41.2 kg, 407.2 mol, 1.1 equiv.) was charged to the reactor, rinsing the transfer line with toluene (25 kg). DPPA (112.2 kg, 407.7 mol, 1.1 equiv.) was charged while maintaining a batch temperature of 10-20 °C and the transfer line was rinsed with toluene (18 kg). The batch was stirred at 10-20 °C for 20 h, and sampled for reaction conversion (result: 5.2% a/a residual SM by HPLC). 10% NaCl (aq) (124 kg, 2 wts.) was charged to the reaction mixture. The batch was stirred for approx. 30 min. at 10-20 °C, then agitation was stopped, and the phases were allowed to separate. The aqueous phase was drained and discarded. The organic phase was washed with 10% NaCl (aq) (126 kg, 2 wts.). The organic phase was dried with anhydrous $MgSO_4$ (25.6 kg, 0.42 wts.) for 2 h (resulting in a residual water content of 0.01% by KF), then the solids were filtered off under nitrogen and the filtrate was collected in a separate appropriately-sized reactor (R2), washing the cake with toluene (91 kg, 1.5 wts.). Toluene (295 kg, 4.8 wts.) was charged to a third reactor (R3), and

stirred. The contents of R2 and R3 were heated to a temperature of 85-95 °C. The reaction mixture was transferred from R2 to R3 over 10.5 h while maintaining the batch temperature in R3 at 85-95 °C, then maintained batch temperature for an additional 2 h. R2 was rinsed with toluene (27.6 kg, 0.5 wts.) and the rinse was added to R3. The batch temperature in R3 was decreased to 55-65 °C and the solution was tested for residual starting material as well as residual azide by ion chromatography (9 ppm; target ≤ 10 ppm; LOQ: 10 ppm). 4 M HCl (aq) (630 kg, 10.2 wts.) was charged to a fourth reactor (R4) and warmed to 85-95 °C. The solution in R3 was transferred to R4 over 10 h while maintaining a batch temperature in R4 of 85-95 °C. R3 was rinsed with toluene (15 kg) and the rinse was added to R4. The batch in R4 was stirred for 1 h, then cooled to 55-65 °C. Stirring was stopped, and the aqueous layer was separated. The aqueous layer was clarified by passing it through an inline filter to remove the emulsion layer, then cooled to 10-20 °C, which resulted in a turbid solution. 40% w/w K_2CO_3 (440 kg, 7.15 wts.) was charged to the batch through a polish filter to a pH of 8-9 (13 h addition time). The batch was stirred for 2 h, then the product was isolated by filtration. The filter cake was washed with 10% w/w Na_2SO_4 (aq) twice (132 kg then 110 kg). The wet cake

was sampled for residual azide (3 ppm; target ≤ 5 ppm). The solids on the filter were dried at 10-20 °C under vacuum for 48 h then at 20-30 °C for 71 h. Yield: 76.85 kg of a solid containing 35% w/w water, and with an overall assay of 48.9% w/w (37.6 kg corrected), corresponding to a 74% corrected yield. ^{1}H NMR (400 MHz, CD_3OD) δ 7.12 (dd, *J* = 4.9 Hz, 1 H), 6.99 (m, 2 H), 4.51 (br d, *J* = 2.8 Hz, 1 H), 3.52 (dd, *J* = 13.9, 3.6 Hz, 1H), 2.87 (br d, *J* = 13.8 Hz, 1H) ppm; ^{13}C NMR (100 MHz, CD_3OD) δ 162.7 (br d, *J* = 242 Hz), 161.4 (br d, *J* = 241 Hz), 159.0 (d, *J* = 2 Hz), 148.4, 147.0 (d, *J* = 7 Hz), 137.9, 137.6 (d, *J* = 3 Hz), 135.2 (d, *J* = 7 Hz), 134.0 (d, *J* = 3 Hz), 132.3 (d, *J* = 8 Hz), 125.1 (d, *J* = 8 Hz), 124.9 (d, *J* = 9 Hz), 117.2 (d, *J* = 22 Hz), 160.0 (d, *J* = 23 Hz), 115.9 (d, *J* = 24 Hz), 112.5 (d, *J* = 23 Hz), 110.2 (d, *J* = 22 Hz), 109.3 (d, *J* = 22 Hz), 66.7, 51.4, 38.7, 37.9, 16.9 ppm; ^{19}F NMR (100 MHz, CD_3OD) δ 115.42 ppm; HRMS: m/z calcd for C_8H_8FN: ($M+H^+$), 138.0714, Found: 138.0716 .

(S)-4-fluorobicyclo[4.2.0]octa-1,3,5-trien-7-amine hemi L-dibenzoyl tartaric acid salt (5•DBTA). Ethanol (151 kg, 4.0 wts.) and L-DBTA (47.2 kg, 0.13 mol, 0.48 equiv.) were charged to an appropriately-sized reactor (R1) and the batch temperature was adjusted

to 15-25 °C. The mixture was stirred for 2 h to dissolve all the solids. Ethanol (19 kg, 0.5 wts.) was charged to R1 to rinse the walls. *rac*-4-Rluorobicyclo[4.2.0]octa-1,3,5-trien-7-amine (**rac 5**; 37.5 kg, 0.27 mol, 1.00 equiv.) was charged to a separate reactor (R2) followed by ethanol (446 kg, 11.9 wts.) and the batch temperature was adjusted to 15-25 °C. The L-DBTA solution from R1 was transferred to R2 over 6 h, and R1 as well as the transfer line were rinsed with ethanol (19 kg, 0.5 wts.), adding the rinse to R2. The batch in R2 was stirred at 15-25 °C for 5 h. The product was isolated by filtration and the solids as well as R2 were rinsed with ethanol (60 kg, 1.6 wts.). The wet cake was reslurried in water (190 kg, 5 wts.) at 15-25 °C for 5 h. The product was isolated by filtration and washed with water (60 kg, 1.6 wts.). The product was dried under vacuum at 35-42 °C for 55 h. Yield: 36.7 kg of a white solid with 98.1% w/w purity, 99.1% a/a purity, and 99.1% *ee* (36 kg corrected), corresponding to a net corrected yield of 41.6%. ^{1}H NMR (400 MHz, DMSO-d6) δ 7.96 (d, *J* = 7.3 Hz, 2 H), 7.60 (m, 1 H), 7.48 (t, *J* = 7.7 Hz, 2 H), 7.11 (m, 3 H), 5.63 (s, 1 H), 4.53 (br d, *J* = 2.8 Hz, 1 H), 3.36 (br dd, *J* = 14.1, 4.0 Hz, 1 H), 2.94 (br d, *J* = 14.3 Hz, 1 H) ppm; ^{13}C NMR (100 MHz, DMSO-d6) δ 167.7, 165.2, 162.4 (br d, *J* = 240 Hz), 161.1 (br d, *J* = 240 Hz), 158.4 (d, *J* = 3 Hz), 148.1 (d, *J*

= 10 Hz), 138.5 (d, *J* = 3 Hz), 135.9 (d, *J* = 7 Hz), 134.6, 133.3 (d, *J* = 8 Hz), 129.9, 129.5, 129.0, 125.9 (d, *J* = 9 Hz), 117.7 (d, *J* = 22 Hz), 116.5 (d, *J* = 23 Hz), 113.1 (d, *J* = 22 Hz), 111.4 (d, *J* = 22 Hz), 66.7(d, *J* = 2 Hz), 38.7, 18.5 ppm; ^{19}F NMR (100 MHz, DMSO) δ 112.87 ppm; HRMS: m/z calcd for C_8H_8FN (free base): ($M+H^+$), 138.0714, Found: 138.0720; $[\alpha]_D^{25}$ = -19.79 (c=1, DMSO).

tert-butyl (Z)-((4-amino-1,2,5-oxadiazol-3-yl)(hydroxyimino)methyl)glycinate (27). To a 10 L 4-neck round-bottomed flask equipped with a mechanical stirrer and maintained under nitrogen, (E)-4-amino-N-hydroxy-1,2,5-oxadiazole-3-carbimidoyl chloride (420 g, 2584 mmol, 1.00 equiv.) and ethyl acetate (4.2 L, 10 vol.) were charged sequentially. Stirring (150 rpm) was initiated and the mixture (a suspension) was cooled to < 5 °C with an ice/water bath. A solution of tert-butyl 2-aminoacetate (373 g, 2842 mmol, 1.10 equiv.) in ethyl acetate (0.525 L, 1.25 vol.) was prepared, and charged to the reaction mixture dropwise over 0.5 h. A solution of triethylamine (392 g, 3876 mmol, 1.50 equiv.) in ethyl acetate (0.525 L, 1.25 vol.) was prepared, and charged to the reaction mixture dropwise over 0.5 h. The resulting solution was stirred for 16 h at ambient temperature,

then sampled for reaction conversion by LCMS analysis. Water (2.5 L, 6.0 vol.) was charged, and phases were allowed to separate. The organic phase was washed with aqueous 1 M hydrochloric acid (1.2 L, 2.85 vol.), then with aqueous 1 M sodium bicarbonate (1.2 L, 2.85 vol.). The organic phase was dried over anhydrous sodium sulfate, filtered, and concentrated to dryness, producing a solid (560 g). The crude solid was slurried in *n*-heptane (2.5 L) and filtered, then dried. Yield: 530 g of a white solid with 82% a/a purity, 70% w/w purity (qNMR[28,29,30]), which corresponds to a 56% yield. ^{1}H NMR (600 MHz, DMSO-d6) δ 10.72 (s, 1H), 6.61 (t, *J* = 6.8 Hz, 1H), 6.32 (s, 2H), 4.06 (d, *J* = 6.9 Hz, 2H), 1.34 (s, 9H) ppm; MS: m/z calcd for $C_9H_{16}N_5O_4$ ($M+H^+$) 258.1, Found 258.1.

(Z)-(4-(N'-hydroxycarbamimidoyl)-1,2,5-oxadiazol-3-yl)glycine (29). To a 10 L 4-neck round-bottomed flask equipped with a mechanical stirrer and maintained under nitrogen, (Z)-tert-butyl 2-(4-amino-N'-hydroxy-1,2,5-oxadiazole-3-carboximidamido)acetate (**27**; 530 g, 1442 mmol, 1.00 equiv.) was charged followed by water (4.24 L, 8 vol.). Stirring (450 rpm) was initiated, and potassium hydroxide (356 g, 6346 mmol, 4.4 equiv.) was

charged at once. The appearance of the mixture gradually changed from a white suspension to an orange solution. The reaction mixture was heated to a batch temperature of 100 °C and maintained for 3.5 days. Reaction conversion was monitored by LCMS analysis. The reaction mixture was cooled to 5 °C, and conc. aqueous hydrochloric acid (12 M, 529 mL, 4.4 equiv.) was charged. The product was isolated by filtration, and washed with water (approx. 0.8 L, twice). The solids were dried in a vacuum oven overnight. Yield: 293.5 g of a white solid with 99% a/a purity, 90% w/w purity (qNMR[28,29,30]), corresponding to a 90% yield. ^{1}H NMR (600 MHz, DMSO-d6) δ 12.90 (s, 1H), 10.54 (s, 1H), 6.43 (t, *J* = 5.6 Hz, 1H), 6.24 (s, 2H), 3.98 (d, *J* = 5.8 Hz, 2H) ppm; MS: m/z calcd for $C_5H_8N_5O_4$ ($M+H^+$) 202.1, Found 202.0.

(Z)-2-(2-((4-(N'-hydroxycarbamimidoyl)-1,2,5-oxadiazol-3-yl)amino)acetamido)ethyl acetate (31). To a 10 L 4-neck round-bottomed flask equipped with a mechanical stirrer and maintained under nitrogen, (Z)-(4-(N'-hydroxycarbamimidoyl)-1,2,5-oxadiazol-3-yl)glycine (**29**; 343 g, 1.53 mol, 1.00 equiv.) and 2-aminoethyl acetate hydrochloride (**30**; 271 g, 1.84 mol, 1.20 equiv.) were charged. THF (6.86 L, 20 vol.) was charged, and the

resulting suspension was stirred at ambient temperature. Diisopropylethylamine (1.61 L, 9.21 mol, 6 equiv.) was charged over 15 min., then stirred for 20 min. at ambient temperature to result in a homogenous light pink suspension. T3P (977 g of a 50% solution in ethyl acetate; 2.46 mol, 1.61 equiv.) was charged over 45 min. The resulting reaction mixture was stirred for 4 h at ambient temperature. Water (4 L, 11.7 vol.) was charged, then the mixture was transferred to a separatory funnel, and the phases were allowed to separate. The aqueous phase was extracted with ethyl acetate (2 L, 5.8 vol.) twice. The organic extracts were combined and washed with brine (1 L), then dried over anhydrous sodium sulfate, filtered, and concentrated under reduced pressure. The solids were re-slurried in ethyl acetate (1 L, 2.9 vol.), filtered, and dried. Yield: 390 g, corresponding to a 80% yield. ^{1}H NMR (600 MHz, DMSO-d6) δ 10.57 (s, 1H), 8.28 (t, *J* = 5.0 Hz, 1H), 6.50 (t, *J* = 5.2 Hz, 1H), 6.21 (s, 2H), 4.01 (t, *J* = 5.5 Hz, 2H), 3.86 (d, *J* = 5.3 Hz, 2H), 3.36 – 3.33 (m, 2H), 2.00 (s, 2H); MS: m/z calcd for $C_9H_{15}N_6O_5$ ($M+H^+$) 287.1, Found 287.1.

(Z)-2-(2-((4-(chloro(hydroxyimino)methyl)-1,2,5-oxadiazol-3-yl)amino)acetamido)ethyl acetate (32). To a 5 L 4-neck round-bottomed flask equipped with a mechanical stirrer and maintained under nitrogen, (Z)-2-(2-((4-(N'-hydroxycarbamimidoyl)-1,2,5-oxadiazol-3-yl)amino)acetamido)ethyl acetate (**31**; 200 g, 0.7 mol, 1.00 equiv), water (1 L), and sodium chloride (122 g, 2.1 mol, 3.00 equiv) were charged sequentially. 6N HCl (1 L, 5 vol.), water (1 L, 5 vol.), and ethyl acetate (1 L, 5 vol.) were then charged sequentially. The reaction mixture was cooled to < 5 °C. Sodium nitrite (50.6 g, 0.73 mol, 1.05 equiv.) was charged as a solution in water (400 mL, 2 vol.) dropwise over 1 h, maintaining a batch temperature of 0-5 °C. After stirring a 0-5 °C for 1 h, the reaction mixture was warmed to ambient temperature. The reaction mixture was transferred to a separatory funnel and the phases were allowed to separate. The aqueous phase was extracted with ethyl acetate (1 L, 5 vol.) three times. The organic extracts were combined and washed with water (2 L, 10 vol.). The organic phase was dried over anhydrous sodium sulfate, filtered and concentrated to dryness under reduced pressure. Yield: 200 g of an off-white solid with 96% w/w purity (qNMR[28,29,30]), corresponding to a 90% yield. Material was used as-is without further purification.

(S,Z)-2-((4-(N-(4-fluorobicyclo[4.2.0]octa-1(6),2,4-trien-7-yl)-N'-hydroxycarbamimidoyl)-1,2,5-oxadiazol-3-yl)amino)-N-(2-hydroxyethyl)acetamide (2). To a 2 L 4-neck round-bottomed flask equipped with a mechanical stirrer and maintained under nitrogen, (S)-4-fluorobicyclo[4.2.0]octa-1,3,5-trien-7-amine hydrochloride (**5•HCl**; 65 g, 374 mmol, 1.00 equiv.) and THF (650 mL, 10 vol.) were charged sequentially. The suspension was stirred and cooled to 0 °C. Solid sodium bicarbonate (79 g, 936 mmol, 2.5 equiv.) was charged, and the resulting mixture was stirred at 0 °C for 5 min. (Z)-2-(2-((4-(chloro(hydroxyimino)methyl)-1,2,5-oxadiazol-3-yl)amino)acetamido)ethyl acetate (**32**; 158 g, 449 mmol, 1.20 equiv.) was dissolved in THF (650 mL, 10 vol.) and the solution was charged to an addition funnel. This solution was added dropwise to the reaction mixture over 1 h, maintaining a batch temperature < 0 °C. After stirring for 3 h at 0 °C, LCMS analysis showed no detectable residual starting material. The reaction mixture was filtered, then diluted with 2-methyltetrahydrofuran (6.5 L, 100 vol.) and water (6.5 L, 100 vol.). The two phases were separated, then the aqueous phase was extracted with 2-methyltetrahydrofuran (2 L, 31 vol.). The organic extracts were combined and dried over anhydrous sodium sulfate,

and concentrated under reduced pressure to approx. 1 L (15 vol.). Then 2-methyltetrahydrofuran (1.3 L, 20 vol.) was charged, and the mixture was concentrated under reduced pressure to approx. 1 L (15 vol.). This operation was repeated two more times (for a total of three solvent exchanges). This resulted in a solution with 0.7% w/w water by KF titration. Methanol (975 mL, 15 vol.) was charged to the mixture, and the suspension was filtered to remove **34**. This resulted in 4000 g (95.5% a/a purity) of a solution that was charged to a 5 L 4-neck round-bottomed flask under nitrogen. Potassium carbonate (46.7 g, 338 mmol, 0.90 equiv.) was charged and the resulting mixture was stirred at ambient temperature for 30 min. Reaction conversion was monitored by HPLC, which showed no remaining ester starting material after 1 h. The reaction mixture was transferred to a separatory funnel and diluted with 2-methyltetrahydrofuran (3 L, 46 vol.) and water (4.5 L, 69 vol.), then mixed to disperse the phases. The phases were separated, and the organic phase was washed with brine (3 L, 46 vol.) four times. The combined aqueous extracts were back-extracted with 2-methyltetrahydrofuran (3 L, 46 vol.), and the organic phases were combined, dried over anhydrous sodium sulfate, and filtered. The organic phase was concentrated under

reduced vacuum to approx. 2 L (approx. 31 vol.). Ethyl acetate (1.5 L, 23 vol.) was charged, and the distillation was repeated down to 2 L (approx. 31 vol.), and the operation was repeated two more times for a total of three solvent exchanges. The resulting suspension was stirred at ambient temperature overnight, and then filtered to afford 105 g of crude **2** (85% yield). Two batches of the crude material were combined and recrystallized by redissolving in THF (18 vol.), then polish-filtered. To the resulting solution, ethyl acetate (15 vol.) was charged, followed by seeding at ambient temperature. After stirring the resulting suspension at ambient temperature for 3 h, the mixture was concentrated under reduced pressure to 10 vol., followed by three additional cycles (add 15 vol. of ethyl acetate and distill) to remove the THF. The resulting suspension was aged overnight at ambient temperature, and filtered and dried to afford **2**. Yield: 165 g of an off-white solid with 99.6% a/a and 99.4% w/w purity and containing 7631 ppm ethyl acetate and 2459 ppm THF. ^{1}H NMR (400 MHz, DMSO-d_6, *ppm*) δ 10.93 (s, 1H), 8.12 (t, J = 5.6 Hz, 1H), 7.16 (dd, J = 8.1, 4.7 Hz, 1H), 7.04 (ddd, J = 10.7, 8.0, 2.3 Hz, 1H), 6.91 (dd, J = 7.9, 2.3 Hz, 1H), 6.74 (d, J = 8.2 Hz, 1H), 6.60 (t, J = 5.4 Hz, 1H), 5.46 (ddd, J = 7.8, 5.1, 2.4 Hz, 1H), 4.66 (t, J = 5.4 Hz, 1H), 3.85 (d,

J = 5.3 Hz, 2H), 3.57 – 3.32 (m, 3H), 3.26 – 2.94 (m, 3H). LC-MS (ES, *m/z*) 365 $[M+H]^+$.

$[\alpha]_D^{20.8}$ = +19.4 ° (c = 0.51, MeOH). *ee* (by SFC) 99.6%.

ASSOCIATED CONTENT

Supporting Information. The following files are available free of charge:

Computational details regarding the energy minimization for the rearrangement (Scheme 6).

AUTHOR INFORMATION

Corresponding Author

*Email: theodore.martinot@infi.com

Present Addresses

⌂Biogen, Inc., Cambridge, Massachusetts, 02142

※Infinity Pharmaceuticals, Inc., Cambridge, Massachusetts, 02139

Notes

The authors declare no competing financial interest.

ACKNOWLEDGMENT

We thank Yaxun Pan, Jianchao Wu, Bin Zhao, Lu Jin, Yanyan Li, Jiannan Huang, Yuxiang Shao and Jing Yang, and Dan Zhou, from WuXi AppTec for support provided on this project. The authors are grateful to LC Campeau for input and review of the manuscript.

ABBREVIATIONS

ARC, accelerating rate calorimetry; AY, assay yield; DCM, dichloromethane; DIPEA, diisopropylethylamine; DoE, design of experiments; DSC, differential scanning calorimetry; IDO-1, Indoleamine-2,3-dioxygenase-1; IY, isolated yield; LCAP, liquid chromatography area percent; PMI, process mass intensity; PTFA, pertrifluoroacetic acid; RAR, rearrangement; SAR, structure-activity relationship; SFC, supercritical fluid chromatography; T3P, propylphosphonic anhydride; TFA, trifluoroacetic acid; THF, tetrahydrofuran; UHP, urea hydrogen peroxide.

REFERENCES

1. Robert, C.; Schachter, J.; Long, G. V.; Arance, A.; Grob, J. J.; Mortier, L.; Daud, A.; Carlino, M. S.; McNeil, C.; Lotem, M.; Larkin, J.; Lorigan, P.; Neyns, B.; Blank, C. U.; Hamid, O.; Mateus, C.; Shapira-Frommer, R.; Kosh, M.; Zhou, H.; Ibrahim, N.; Ebbinghaus, S.; Ribas, A. Pembrolizumab versus Ipilimumab in Advanced Melanoma, *N. Engl. J. Med.* **2015**, *372*, 2521−2532.

2. Munn, D. H.; Zhou, M.; Attwood, J. T.; Bondarev, I.; Conway, S. J.; Marshall, B.; Brown, C.; Mellor, A. L. Prevention of Allogeneic Fetal Rejection by Tryptophan Catabolism, *Science* **1998**, *281*, 1191−1193.

3. Munn, D. H.; Mellor, A. L. IDO and tolerance to tumors, *Trends Mol. Med.* **2004**, *10* (1), 15−18.

4. Uyttenhove, C.; Pilotte, L.; Theate, I.; Stroobant, V.; Colau, D.; Parmentier, N.; Boon, T.; Van den Eynde, B. J. Evidence for a tumoral immune resistance mechanism based on tryptophan degradation by indoleamine 2,3-dioxygenase, *Nat. Med.* **2003**, *9*, 1269−1274.

5. Spranger, S.; Horton, B.; Koblish, H. K.; Scherle, P. A.; Newton, R.; Gajewski, T. F. Mechanism of tumor rejection with doublets of CTLA-4, PD-1/PD-L1, or IDO blockade

involves restored IL-2 production and proliferation of CD8(+) T cells directly within the tumor microenvironment, *J. Immunother. Cancer* **2014**, *2*, 3.

6. (a) Yue, E. W.; Sparks, R.; Polam, P.; Modi, D.; Douty, B.; Wayland, B.; Glass, B.; Takvorian, A.; Glenn, J.; Zhu, W.; Bower, M.; Liu, X.; Leffet, L.; Wang, Q.; Bowman, K. J.; Hansbury, M. J.; Wei, M.; Li, Y.; Wynn, R.; Burn, T. C.; Combs, A. P. INCB24360 (Epacadostat), a Highly Potent and Selective Indoleamine-2,3-dioxygenase 1 (IDO1) Inhibitor for Immuno-oncology, *ACS Med. Chem. Lett.* **2017**, *8*, 486-491. (b) Yue, E. W.; Douty, B.; Wayland, B.; Bower, M.; Liu, X.; Leffet, L.; Wang, Q.; Bowman, K. J.; Hansbury, M. J.; Liu, C.; Wei, M.; Li, Y.; Wynn, R.; Burn, T. J.; Koblish, H. K.; Fridman, J. S.; Metcalf, B.; Scherle, P.; Combs, A. P. Discovery of Potent Competitive Inhibitors of Indoleamine 2,3-Dioxygenase with in Vivo Pharmacodynamic Activity and Efficacy in a Mouse Melanoma Model, *J. Med. Chem.* **2009**, *52*, 7364-7367.

7. (a) Liu, K.; Achab, A.; Biju, P.; Cernak, T. A.; Deng, Y.; Fradera, X.; Guo, L.; Han, Y.; He, S.; Kozlowski, J.; Li, D.; Li, G.; Pu, Q.; Shi, Z.-C.; Yu, W.; Zhang, H. Novel substituted *N*-hydroxycarbamimidoyl-1,2,5-oxazole compounds as indoleamine 2,3-dioxygenase (IDO) inhibitors and their preparation. WO 2018044663A1, March 8, 2018.

(b) Zhang, H.; Achab, A.; Ardolino, M.; Chai, X.; Cheng, M.; Deng, Y.; Doty, A.; Ferguson, H.; Fradera, X.; Knemeyer, I.; Li, C.; Liu, K.; Martinot, T.; McGowan, M. A.; Miller, R.; Otte, K.; Pu, Q.; Purakattle, B.; Sciammetta, N.; Solban, N.; Song, X.; Spacciapoli, P.; Wise, A.; Yu, W.; Zhou, H.; Bennett, D.; Han, Y. Discovery and optimization of potent, selective, and orally available IDO1 heme-binding inhibitors featuring a novel A-pocket piece. *Abstracts of Papers, 256th ACS National Meeting & Exposition*, Boston, MA, United States, August 19-23, 2018.

8. Compound **6** is also often referred to as ACOF in the literature, which primarily centers around the formation of high energy materials. For examples of synthetic access and application of this building block, see: (a) Tsyshevsky, R.; Pagoria, P.; Zhang, M.; Racoveanu, A.; Parrish, D. A.; Smirnov, A. S.; Kuklja, M. M. Comprehensive End-to-End Design of Novel High Energy Density Materials: I. Synthesis and Characterization of Oxadiazole Based Heterocycles, *J. Phys. Chem. C* **2017**, *121*, 23853-23864. (b) Pagoria, P. F.; Zhang, M.-X.; Zuckerman, N. B.; DeHope, A. J.; Parrish, D. A. Synthesis and characterization of multicyclic oxadiazoles and 1-hydroxytetrazoles as energetic materials, *Chemistry of Heterocyclic Compounds* **2017**,

53, 6/7, 760-778. (c) Tang, Y.; He, C.; Shreeve, J. M. A furazan-fused pyrazole N-oxide via unusual cyclization, *J. Mater. Chem. A* **2017**, *5*, 4314-4319. (d) Yu, Q.; Cheng, G.; Ju, X.; Lu, C.; Lin, Q.; Yang, H. An interesting 1,4,2,5-dioxadiazine-furazan system: structural modification by incorporating versatile functionalities, *Dalton Trans.* **2017**, *46*, 14301-14309. (e) Huang, H.; Li, Y.; Yang, J.; Pan, R.; Lin, X. Materials with good energetic properties resulting from the smart combination of nitramino and dinitromethyl group with furazan, *New J. Chem.* **2017**, *41*, 7697-7704. (f) Li, Y.; Huang, H.; Shi, Y.; Yang, J.; Pan, R.; Lin, X. Potassium nitraminofurazan derivatives: Potential green primary explosives with high energy and comparable low friction sensitivities, *Chem. Eur. J.* **2017**, *23*, 7353-7360. (g) Duddu, R.; Hoare, J.; Sanchez, P.; Damavarapu, R.; Parrish, D. Synthesis of nitro, dinitro, and polynitroalkylamino derivatives of trifurazanoxide, *J. Heterocyclic Chem.* **2017**, *54*, 3087-3092. (h) Austin, C. J. D.; Moir, M.; Kahlert, J.; Smith, J. R.; Jamie, J. F.; Kassiou, M.; Rendina, L. M. Carborane-containing hydroxyamidine scaffolds as novel inhibitors of indoleamine 2,3-dioxygenase 1 (IDO1), *Aust. J. Chem.* **2015**, *68*, 1866-1870.

9. Agosti, A.; Bertolini, G.; Bruno, G.; Lautz, C.; Glarner, T.; Deichtmann, W. Handling hydrogen peroxide oxidations on a large scale: Synthesis of 5-bromo-2-nitropyridine, *Org. Process Res. Dev.* **2017**, *21*, 3, 451-459.

10. For examples of additions of nucleophiles to nitrooxadiazoles, see: (a) Blangetti, M.; Rolando, B.; Chegaev, K.; Guglielmo, S.; Lazzrato, L.; Durante, M.; Masini, E.; Almirante, N.; Bastia, E.; Impagnatiello, F.; Fruttero, R.; Gasco, A. New furoxan derivatives for the treatment of ocular hypertension, *Bioorg. Med. Chem. Lett.* **2017**, *27*, 479-483. (b) Qu, X.-N.; Zhang, S.; Wang, B.-Z.; Yang, Q.; Han, J.; Wei, Q.; Xie, G.; Chen, S.-P. An Ag(I) energetic metal–organic framework assembled with the energetic combination of furazan and tetrazole: synthesis, structure and energetic performance, *Dalton Trans.* **2016**, *45*, 6968-6973. (c) Stepanov, A. I.; Sannikov, V. S.; Dashko, D. V.; Roslyakov, A. G.; Astrat'ev, A. A.; Stepanova, E. V. A new preparative method and some chemical properties of 4-R-furazan-3-carboxylic acid amidrazones, *Chemistry of Heterocyclic Compounds* **2015**, *51*, 4, 350-360. (d) Chegaev, K.; Lazzrato, L.; Tamboli, Y.; Boschi, D.; Blangetti, M.; Scozzafava, a.; Carta, F.; Masini, E.; Fruttero, R.; Supuran, C. T.; Gasco, A. Furazan and furoxan sulfonamides are strong α-carbonic anhydrase

inhibitors and potential antiglaucoma agents, *Bioorg. Med. Chem.* **2014**, *22*, 3913-3921. (e) Paton, R. M. Product Class 7: 1,2,5-Oxadiazoles. In *Science of Synthesis 13: Category 2, Hetarenes and Related Ring Systems*; Storr, R. C.; Gilchrist, T. L., Eds.; Thieme: New York, **2004**; Vol. 13, pp. 185-218. (f) Boschi, D.; Sorba, G.; Bertinaria, M.; Fruttero, R.; Calvino, R.; Gasco, A. Unsymmetrically substituted furoxans. Part 18. Smiles rearrangement in furoxan systems and in related furazans, *J. Chem. Soc., Perkin trans. 1* **2001**, 1751-1757.

11. Refer to the "rule of six" cited in Kolb, H. C., Finn, M. G., Sharpless, K. B. Click chemistry: Diverse chemical function from a few good reactions, *Angew. Chem. Int. Ed.* **2001**, *40*, 2004-2021.

12. Bassan, E.; Ruck, R. T.; Dienemann, E.; Emerson, K. M.; Humphrey, G. R.; Raheem, I. T.; Tschaen, D. M.; Vickery, T. P.; Wood, H. B.; Yasuda, N. Merck's reaction review policy: An exercise in process safety, *Org. Process Res. Dev.* **2013**, *17*, 1611-1616.

13. *Recommendations on the Transport of Dangerous Goods, Manual of Tests and Criteria, Fifth Revised Edition*. ST/SG/AC.10/11/Rev.5. United Nations: New York, 2009.

14. Stoessel, F. Planning protection measures against runaway reactions using criticality classes, *Process Safety Env. Prot.* **2009**, *87*, 2, 105-112.

15. Mel'nikova, T. M.; Novikova, T. S.; Khmel'nitskii, L. I.; Sheremetev, A. B. Novel synthesis of 3,4-dicyanofuroxan, *Mendeleev Commun.* **2001**, *11*, 1, 30-31.

16. 4471. Hydrogen peroxide. *Bretherick's Handbook of Reactive Chemical Hazards,* 7th ed.; Elsevier: Oxford, UK, 2007; pp. 1692 – 1712. Refer specifically to the entry on p. 1710 for sulfuric acid.

17. 0661. Trifluoroacetic acid. *Bretherick's Handbook of Reactive Chemical Hazards,* 7th ed.; Elsevier: Oxford, UK, 2007; p. 285.

18. 0475a. Urea hydrogen peroxidate. *Bretherick's Handbook of Reactive Chemical Hazards,* 7th ed.; Elsevier: Oxford, UK, 2007; p. 213.

19. 0662. Peroxytrifluoroacetic acid. *Bretherick's Handbook of Reactive Chemical Hazards,* 7th ed.; Elsevier: Oxford, UK, 2007; p. 286.

20. Caster, K. C.; Rao, A. S.; Mohan, H. R.; McGrath, N. A.; Brichacek, M. Trifluoroperacetic Acid, *e-EROS Encyclopedia of Reagents for Organic Synthesis* **2012**.

21. Benassi, R.; Taddei, F. Thermochemical properties and homolytic bond cleavage of organic peroxyacids and peroxyesters: an empirical approach based on ab initio MO Calculations, *J. Mol. Struct. (Theochem)* **1994**, *303*, 101-117.

22. Shaposhnikov, S. D.; Romanova, T. V.; Spiridonova, N. P.; Mel'nikova, S. F.; Tselinskii, I. V. Some Reactions of 3,6-Bis(4-amino-1,2,5-oxadiazol-3-yl)-1,4,2,5-dioxadiazine, *Rus. J. Org. Chem.* **2004**, *40*, 6, 884-888.

23. Leonard, P. W.; Pollard, C. J.; Chavez, D. E.; Rice, B. M.; Parrish, D. A. 3,6-Bis(4-nitro-1,2,5-oxadiazol-3-yl)-1,4,2,5-dioxadiazene (BNDD): A Powerful Sensitive Explosive, *Synlett* **2011**, *14*, 2097-2099.

24. Ghislandi, V.; Vercesi, D. Scissione ottica e configurazione dell'1-aminobenzociclobutene e dell'1-aminoindano, *Boll. Chim. Farm.* **1978**, *115*, 489-500.

25. Liu, J.; Kolar, C.; Lawson, T. A.; Gmeiner, W. H. Targeted Drug delivery to chemoresistant cells: Folic acid derivatization of FdUMP[10] enhances cytotoxicity toward 5-FU-resistant human colorectal tumor cells, *J. Org. Chem.* **2001**, *66*, 5655-5663.

26. Sperry, J. B.; Minteer, C. J.; Tao, J. Y.; Johnson, R.; Duzguner, R.; Hawksworth, M.; Oke, S.; Richardson, P. F.; Barnhart, R.; Bill, D. R.; Giusto, R. A.; Weaver, J. D. III. Thermal stability assessment of peptide coupling reagents commonly used in pharmaceutical manufacturing, *Org. Process Res. Dev.* **2018**, *22*, 9, 1262-1275.

27. JMP 12.1.10 (32-bit), SAS Institute, Inc.

28. Yang, Q.; Qiu, H.; Guo, W.; Wang, D.; Zhou, X.; Xue, D.; Zhang, J.; Wu, S.; Wang, Y. Quantitative ^{1}H-NMR Method for the Determination of Tadalafil in Bulk Drugs and its Tablets, *Molecules* **2015**, *20*, 7, 12114-12124.

29. Malz, F.; Jancke, H. Validation of quantitative NMR, *J. Pharm. Biomed. Anal.* **2005**, *38*, 5, 813-823.

30. A qNMR pulse sequence (Bruker) with the following parameters was used: zg30 with d1 = 60 s.